ResearchGate

See discussions, stats, and author profiles for this publication at: https://www.researchgate.net/publication/229315192

Electrochemical reduction of oxygen and hydrogen peroxide catalyzed by a surface copper(II)–2,4,6-tris(2-piridil)-1,3,5-triazine complex adsorbed on a graphite electrode

ARTICLE *in* JOURNAL OF POWER SOURCES · MARCH 2005

Impact Factor: 6.22 · DOI: 10.1016/j.jpowsour.2004.09.032

CITATIONS
38

READS
116

6 AUTHORS, INCLUDING:

Marques Edmar Pereira
Universidade Federal do Maranhão
30 PUBLICATIONS **851** CITATIONS
SEE PROFILE

Jiujun Zhang
National Research Council Canada
241 PUBLICATIONS **12,024** CITATIONS
SEE PROFILE

Aldaléa L.B. Marques
Universidade Federal do Maranhão
29 PUBLICATIONS **945** CITATIONS
SEE PROFILE

Available from: Aldaléa L.B. Marques
Retrieved on: 23 January 2016

Available online at www.sciencedirect.com
SCIENCE DIRECT®
Journal of Power Sources 142 (2005) 10–17
JOURNAL OF POWER SOURCES
www.elsevier.com/locate/jpowsour

Electrochemical reduction of oxygen and hydrogen peroxide catalyzed by a surface copper(II)–2,4,6-tris(2-piridil)-1,3,5-triazine complex adsorbed on a graphite electrode

Vera L.N. Dias[a], Elizabeth N. Fernandes[a], Leila M.S. da Silva[a], Edmar P. Marques[a], Jiujun Zhang[b], Aldaléa L. Brandes Marques[a,*]

[a] *Department of Technology Chemistry, Federal University of Maranhão, Av. dos Portugueses, S/N, Campus do Bacanga, São Luis 65080-040, MA, Brazil*
[b] *Institute for Fuel Cell Innovation, National Research Council Canada, Vancouver, BC, Canada V6T 1W5*

Received 31 August 2004; accepted 22 September 2004
Available online 30 December 2004

Abstract

A graphite electrode irreversibly adsorbed by 2,4,6-tris(2-piridil)-1,3,5-triazine (abbreviated as TPT) was examined by cyclic voltammetry. The adsorbed TPT exhibited two irreversible reduction waves in the potential range of −0.7 and −1.0 V (versus SCE). Upon strong adsorption, TPT can serve as a coordination ligand for copper ions to form a surface complex. Its three adjacent nitrogen positions provide strong affinity to the metal ions and bond copper(II) to an electrode surface. A 1:1 coordination between Cu(II) or Cu(I) and the TPT ligand to form $[Cu(II)(TPT)]^{2+}$ or $[Cu(I)(TPT)]^{+}$ is the predominant process, evidenced by spectrophotometry, surface cyclic voltammetry, and coordinated structural feasibility of Cu(II)/Cu(I)–TPT complexes. The predominant copper(II)–TPT surface complex shows a reversible redox wave, which is identified as one-electron process of $[Cu(II)(TPT)]^{2+} \leftrightarrow [Cu(I)(TPT)]^{+}$.

The electrode adsorbed by $[Cu(II)(TPT)]^{2+}$ complex showed electrocatalytic activity towards oxygen and/or hydrogen peroxide reductions. The catalyzed reduction of oxygen and hydrogen peroxide were identified as four-electron and two-electron process to form water. It is suggested that the possible electrocatalytic reductions were due to an inner-sphere mechanism, which involved a coordination between substrate (O_2 or H_2O_2) and $[Cu(I)(TPT)]^{+}$. The reduction kinetics were also investigated by a rotating disk electrode method.
© 2004 Elsevier B.V. All rights reserved.

Keywords: Graphite electrode; 2,4,6-Tris(2-piridil)-1,3,5-triazine; Copper complex; Electrocatalysis; Oxygen reduction; Hydrogen peroxide reduction

1. Introduction

Electrode surface attachment by an active molecule or a functional group has drawn great attention in the recent years due to its fundamental importance in understanding the mechanisms of surface electron transfer, surface structural effects, and electrochemical catalysis [1,2].

The adsorption process of irreversibly-adsorbed organic molecules with large conjugated aromatic rings, such as anthraquinones [3], phenanthrolines [4–10] and triazines [9–11] has been used to create electrode surfaces with electroactive and chelating groups for the purpose of chemical analysis and surface electrocatalysis. Electrode surfaces attached by a metal complex formed between an irreversibly-adsorbed ligand and a metal ion have been also explored for the purpose of electrocatalytic reduction of oxygen and hydrogen peroxide, which is fundamentally important to low-cost catalyst development in energy devices such as fuel cells [1,2,10–12].

In this paper, the surface electrochemistry of adsorbed 2,4,6-tris(2-piridil)-1,3,5-triazine (TPT) and its surface complex with copper ions (Cu(II)–TPT or Cu(I)–TPT) are reported. The electrocatalytic activity of a surface copper–TPT complex adsorbed on a graphite electrode towards the O_2 and

* Corresponding author. Tel.: +55 98 217 8299; fax: +55 98 217 8245.
E-mail address: aldalea@uol.com.br (A.L.B. Marques).

0378-7753/$ – see front matter © 2004 Elsevier B.V. All rights reserved.
doi:10.1016/j.jpowsour.2004.09.032

H_2O_2 reduction is also investigated. The kinetics of electrocatalyzed O_2 or/and H_2O_2 reduction are examined by cyclic voltammetric and rotating disk electrode methods. The possible reaction mechanisms are also discussed.

2. Experimental

2.1. Reagents and materials

All reagents ($Cu(SO_4)_2{\cdot}5H_2O$ (Merck), 2,5,6-tris(2-piridil)-1,3,5-triazine (Aldrich), $NaClO_4$ (Merck), H_3PO_4 (Merck), H_3BO_3 (Merck), NaOH (Merck) and 30% H_2O_2 aqueous solution (Merck) were analytical grade, and used without further purification. For solution preparation, double-distilled water was further purified through an ultra-purification system (NANOPURE Water System, model D4741). Britton–Robinson buffer solutions (abbreviated as BR buffer; $CH_3COOH + H_3BO_3 + H_3PO_4$, 0.04 mol dm^{-3} for each component) containing 0.1 mol dm^{-3} of $NaClO_4$ were used as supporting electrolyte. The pH adjustment was obtained with addition of 1.0 mol dm^{-3} NaOH to the supporting electrolyte. Nitrogen gas with high purity of 99.99% was used to bubble through the test solution to remove dissolved oxygen.

2.2. Electrode preparation

Pyrolytic graphite electrodes were sealed to stainless steel shafts with heat shrinkable polyolefin tubing. Electrodes were mounted with the basal planes of the graphite exposed but the polishing procedure could result in edge plane exposure. The electrode area was 0.16 cm^2, which was calibrated electrochemically by a 1×10^{-3} mol dm^{-3} solution of $K_3[Fe(CN)_6]$. Electrodes were polished using 0.5 μm alumina, sonicated for 10 min in water and rinsed with acetone and water before each experiment.

2.3. Electrochemical measurements

Electrochemical measurements were performed by a conventional three-compartment, three-electrode cell. A saturated calomel electrode (SCE) was used as the reference electrode, and a platinum wire as the auxiliary electrode, respectively. Cyclic voltammetry was conducted with an electrochemical analyzer PAR 164 A. For rotating disk voltammetry, an RDE3 potentiostat and ARS rotator (Pine Instruments) were employed with an *X–Y* recorder. For oxygen reduction experiments, the electrolyte was bubbled with pure O_2 for at least 15 min. The dissolved oxygen concentration was taken as 1.3×10^{-3} mol dm^{-3} at ambient conditions.

2.4. Surface attachment

For TPT attachment, a polished electrode was inserted into a 1×10^{-3} mol dm^{-3} TPT aqueous solution for a period of 10–30 s, taken out and rinsed with water, then transferred to an electrochemical cell containing only the supporting electrolyte for measurement. For surface Cu(II)–TPT complex formation, the electrode previously coated with TPT was exposed to a solution of 1×10^{-4} mol dm^{-3} $CuSO_4$ for 10–30 s, taken out and washed with water for electrochemical measurement.

All experiments were conducted at ambient laboratory temperature ($25 \pm 2\,^{\circ}C$). Potentials were measured with respect to a saturated calomel electrode.

3. Results and discussion

3.1. Surface electrochemistry of TPT

As shown in Fig. 1, TPT is a large conjugated molecule, capable of inducing a strong and irreversible adsorption on a graphite electrode. Fig. 2 shows the surface cyclic voltammetry of adsorbed TPT on a graphite electrode (b). For the purpose of comparison, the cyclic voltammetry for the bare graphite surface was also recorded as shown in Fig. 2(a). There are two irreversible reduction waves (waves I and II), which were observed near the potentials of −0.72 and −1.01 V. In order to see the reversibility of wave I, the potential was scanned to −0.85 V, then scanned back. In this way, the further reduction (wave II) was avoided. No reversible oxidation wave was observed, indicating that the electrochemical process for wave I is an irreversible reduction.

The area under wave II is about 1.8 times larger than that of wave I. This suggests that the electron number involving in wave II may be two times greater than that of wave I. In order to know how many electrons were contained in the waves, the graphite electrode was coated with various known quantities of TPT ($\sim 10^{-11}$ mol cm^{-2}) and then inserted into the pure supporting electrolyte (pH 5.3, BR buffered) to record the cyclic voltammograms [13]. In this way, two distinguishable waves similar to those in Fig. 2 were obtained. However, wave II became very broad and flat, which made the area determination difficult. The difference between the dry coating and the wet adsorption for the electrode modification may be responsible for the distortion of wave II. Wave I was still in a well-defined shape, from which the electron number of 1.9 was obtained. This number of 1.9 suggested that wave I was a two-electron reduction process. Combined with the

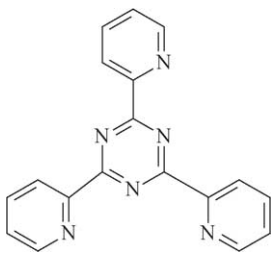

Fig. 1. Molecular structure of 2,5,6-tris(2-piridil)-1,3,5-triazine (TPT).

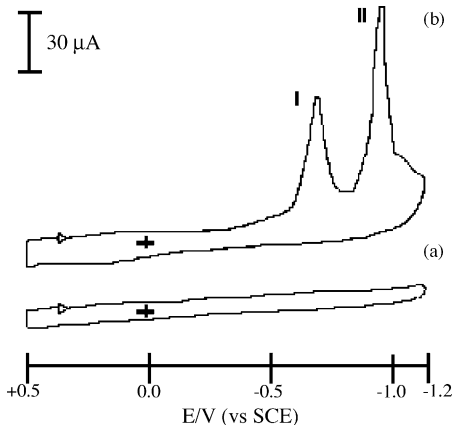

Fig. 2. Voltammetric responses of a bare graphite electrode (a) and a TPT adsorbed graphite electrode (b). The cleaned electrode was first exposed into a TPT solution for 25 s, then washed and transferred to a solution containing only supporting electrolyte (0.1 mol dm^{-3} $NaClO_4$); Britton–Robinson buffer: 0.04 mol dm^{-3} $CH_3COOH/H_3BO_3/H_3PO_4$, pH 5.3. Potential scan rate: 100 mV s^{-1}. TPT surface concentration: 9.97×10^{-10} mol cm^{-2}.

observation in Fig. 2 that the area of wave II was twice that of wave I, it may be concluded that wave II is a four-electron process. This observation is consistent with the results concluded by Kamal et al. [14] on a mercury electrode. Fig. 3 shows the results for the wave potential pH dependences in the range of 2.0–8.0. Both peak potentials moved in the negative direction with the pH increase. When the pH was higher than 8.0, the waves became too broad and flat, which made the peak potential measurement unreliable. The linear relationship between the wave peak potential and the solution pH both had a slope ~60 mV pH^{-1}. This is close to a theoretical value of 58 mV pH^{-1} for a half electrochemical reaction involving a 1:1 ratio of electron and proton numbers. It may be concluded that the reduction of wave I involves two protons and two electrons, and the reduction of wave II involves four protons and four electrons. Kamal et al. [14] have given the explanation of TPT reduction process on a mercury electrode surface. The total of six electrons and six protons would go to the middle triazine ring to covert three double bonds into three single bonds, destroying the conjugate structure of TPT molecule. The reduction of wave I converted the first double bond into a single bond, and the wave II did the other two.

3.2. Surface electrochemistry of adsorbed Cu(II)/Cu(I)–TPT complexes

The electrode adsorbed by TPT was transferred to a solution containing 4×10^{-5} mol dm^{-3} of Cu(II), and then scanned between the potentials of 0.5 and −0.6V for 15 cycles at a potential scan rate of 100 mV s^{-1}. After that step, the electrode was taken out, transferred into a solution only containing supporting electrolyte for surface electrochemical measurement. The obtained cyclic voltammogram as shown in Fig. 4 (b) from which the surface responses of surface Cu(II)/Cu(I)–TPT complexes can be observed compared to that of a bare graphite electrode surface (Fig. 4(a)). Similar behavior has been reported in [7] for a Cu(II) surface complex although the ligand employed in that paper is different from the one used in the present work. It is believed that the response (waves III/III′) is an electrochemical process of the surface Cu(II)–TPT complex which has a 1:1 ratio between the metal center and the ligand. The copper may undergo a one-electron reduction/oxidation between Cu(II) and Cu(I).

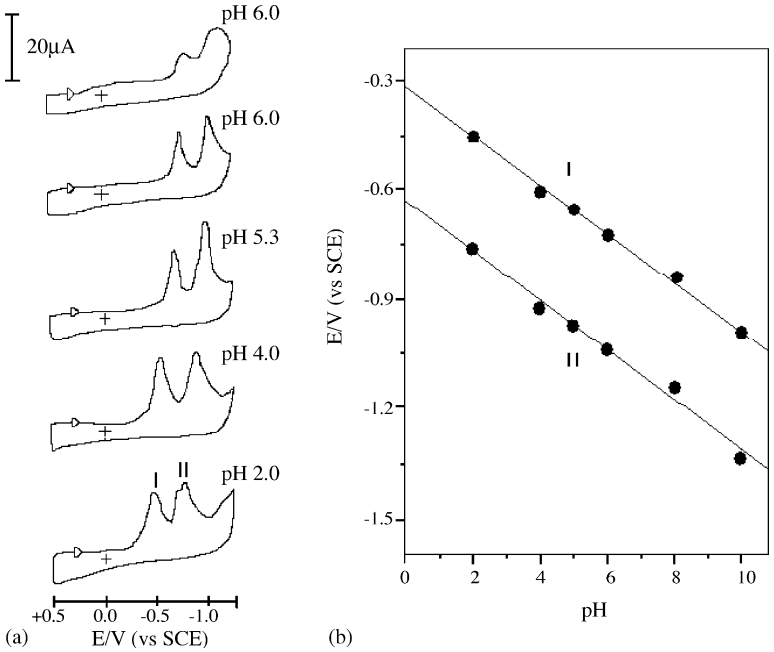

Fig. 3. (a) Cyclic voltammograms of adsorbed TPT on the graphite electrode surface. Experimental conditions are as in Fig. 2. (b) Peak potential as a function of solution pH (data from (a)).

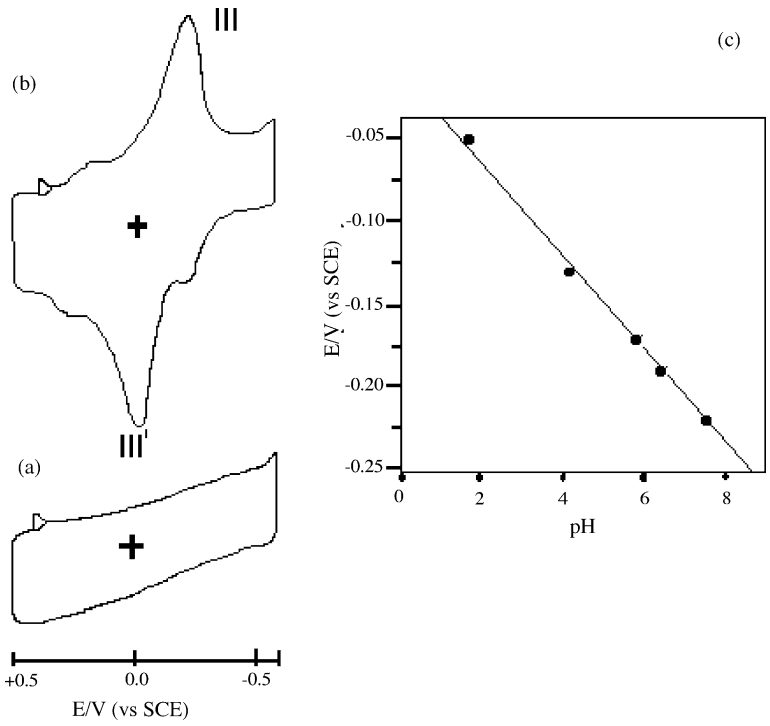

Fig. 4. Cyclic voltammograms of a bare graphite electrode (a) and a Cu(II)–TPT-coated graphite electrode (b). (c) The pH dependency of waves III/III′ in (b). Experimental conditions are as in Fig. 2.

The pH dependence of the average peak potential was also obtained by adjusting the solution pH in the range of 0–6. The linear relationship had a slope of ∼48 mV pH^{-1} which could be considered to be close to the theoretical value of 58 mV for a half electrochemical reaction involving a 1:1 ratio of electron and proton numbers. Thus, the result suggests that the surface reduction/oxidation of the copper center involved one electron and one proton. The reaction could be expressed as the follows:

$$[Cu(II)TPT(H_2O)_2(OH)]^+ + H^+ + e^- \leftrightarrow [Cu(I)TPT(H_2O)]^+ + 2H_2O \quad (1)$$

dIn general, Cu(II) favors a coordination number of 6, and Cu(I) complexes favors a coordination number of 4. In each TPT molecule, there are three nitrogen positions available with which a Cu(II) or Cu(I) ion can coordinate.

In the case of Cu(II), as discussed in Section 3.3, each Cu(II) center could only take one TPT molecule in the coordination process, indicating that for total six coordination positions around the Cu(II) center, three of them are occupied by TPT, and other three by one OH^- group and two water molecules. The observation that the Cu(II) center cannot be able to coordinate with two TPT molecules may be understood based on the steric effect of the large sized TPT molecule. In the case of Cu(I), each Cu(I) could take one TPT ligand, and the fourth position would be occupied by H_2O molecule. The proposed surface complex of Cu(II)/Cu(I) are as shown in Fig. 5.

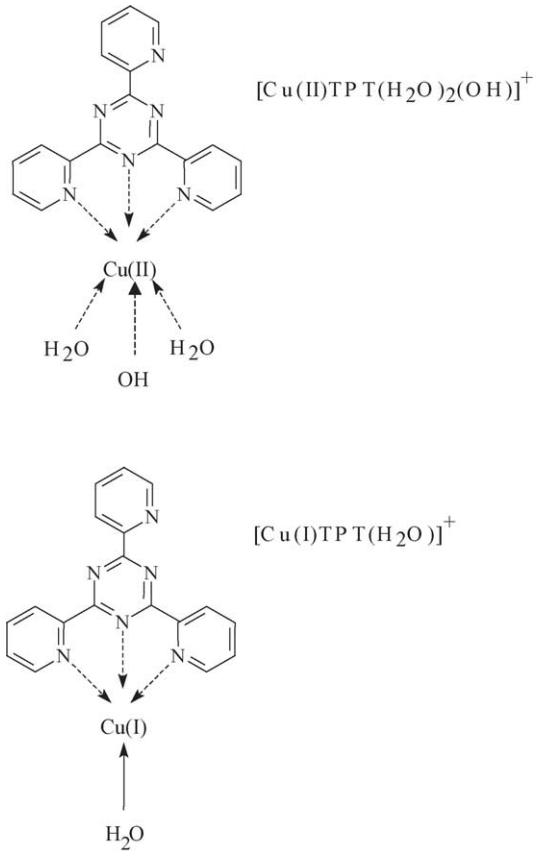

Fig. 5. Proposed molecular structures of Cu(II)/Cu(I)–TPT complexes.

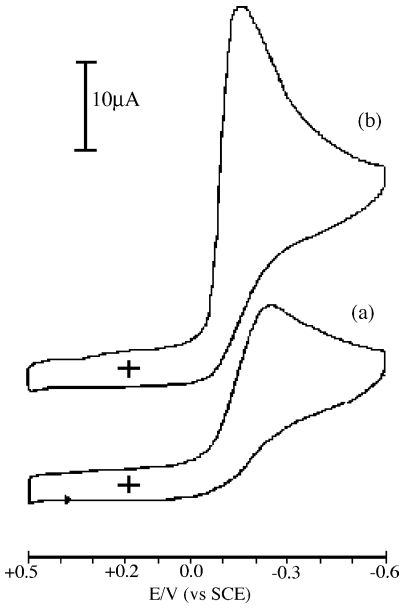

Fig. 6. Cyclic voltammograms of H_2O_2 (a) and O_2 (b) reductions electrocatalyzed by a Cu(II)–TPT complex adsorbed on the graphite electrode. The concentration for both O_2 and H_2O_2 is 2.4×10^{-4} mol dm^{-3}. Other experimental conditions are as in Fig. 2.

Several solutions containing different mole ratios of Cu(II) and TPT ligand (the total concentration of Cu(II) + TPT was in the range of 1×10^{-3} to 1×10^{-2} mol dm^{-3}) were measured by an UV–vis spectroscopic method. The purpose of this experiment was to confirm that the complex reaction between Cu(II) with TPT was 1:1 coordination as proposed on the graphite electrode surface above. The aqueous solution for the complexes of Cu(II) with TPT shows a maximum absorbance at the wavelength of 288 nm. The continuous variation plots (absorbance at 288 nm versus the concentration of [Cu(II)]/([Cu(II)] + [TPT]), gave a maximum absorbance at ∼1.0, suggesting that the complex reaction between Cu(II) and TPT ligand indeed favors the 1:1 coordination.

3.3. Electrocatalytic activities of $[Cu(II)TPT]^{2+}$ toward the reduction of O_2 and H_2O_2

The graphite electrode modified by Cu(II)–TPT complex was tested in an air saturated solution (pH 5.3, O_2 concentration is approximately 2.4×10^{-4} mol dm^{-3}). It was separately tested for electrocatalytic activity in a solution containing 2.4×10^{-4} mol dm^{-3} of H_2O_2. For the comparison, the bare electrode was also tested in the same way. Compared to the bare electrode, a significant current enhancement for both O_2 and H_2O_2 reductions was observed on the Cu(II)–TPT modified electrode. Fig. 6 shows the cyclic voltammonograms of H_2O_2 (a) and O_2 (b) reductions. Both catalyzed reduction peak potentials were near the formal potentials of the waves III/III′, indicating that Cu(II)/Cu(I)–TPT was responsible for the catalytic process. For a proposed reduction mechanism, see Section 3.4.

The magnitude of the current for O_2 reduction is almost double that of H_2O_2 reduction, suggesting that the electron number involved in the catalyzed O_2 reduction may be two times more that for H_2O_2 reduction. As proven in this paper, the catalyzed O_2 reduction by Cu(II)–TPT undergoes a four-electron process to form water:

$$O_2 + 4H^+ + 4e^- \rightarrow 2H_2O \quad (2)$$

and H_2O_2 reduction is through a two-electron process to H_2O:

$$H_2O_2 + 2H^+ + 2e^- \rightarrow 2H_2O \quad (3)$$

For a quantitative estimation of the reduction process, the two catalyzed reductions were also examined with a rotating disk electrode on which Cu(II)-TPT was adsorbed. Fig. 7 shows the current–potential curves at various rotating rates for the reduction of O_2 (a) and H_2O_2 (c) at a rotating Cu(II)-TPT modified electrode together with their corresponding Koutecky–Levich plots ((b) for O_2 and (d) for H_2O_2). The dashed lines are those calculated according to Koutecky–Levich theory for the four-electron reduction of O_2 and two-electron reduction of H_2O_2 with a fully diffusion controlled assumption. The observation from Fig. 7(b) and (d) that the experimental linear lines for both cases are parallel to those calculated for four-electron and two-electron processes, suggest that the catalyzed O_2 reduction was a four-electron process (expressed as in Eq. (2)), and the catalyzed H_2O_2 reduction was a two-electron process (expressed in Eq. (3)). The non-zero intercepts for both cases in Fig. 7(b) and (d) indicated that the reduction of O_2 and H_2O_2 catalyzed by a Cu(II)/Cu(I)-TPT/electrode were controlled by a chemical step. The intercept of Koutecky–Levich plot can be expressed as [8,11]:

$$\frac{1}{I_k} = \frac{1}{nFAkC\Gamma} \quad (4)$$

where n is the overall electron number of corresponding reduction (for O_2, $n = 4$, and for H_2O_2, $n = 2$), F is the Faraday's constant, A is the electrode surface, k is the rate constant governing the reaction of the catalyst, C is the concentration of O_2 or H_2O_2, and Γ is the quantity of the catalyst on the electrode that participates in the catalyzed reaction.

The values of I_k were obtained at a Cu(II)–TPT surface concentration of 7.5×10^{-10} mol cm^{-2} by adjusting the concentration of O_2 or H_2O_2, as shown in Fig. 8(a) and (c) , respectively. The linear relationship between I_k and the concentration suggests that both O_2 and H_2O_2 have a reaction

Table 1
Rate constants for O_2 reduction catalyzed by Cu(II)–TPT/electrode at 25 °C and 1.0 atm

$C(O_2)$ ($\times 10^4$ mol dm^{-3})	I_k (μA)	$k(O_2)$ ($\times 10^{-5}$ mol^{-1} dm^3 s^{-1})
1.8	4.1	9.4
2.7	6.3	9.5
3.6	7.8	8.9
4.5	9.6	8.7

The Cu(II)–TPT surface concentration is 7.5×10^{-10} mol cm^{-2}.

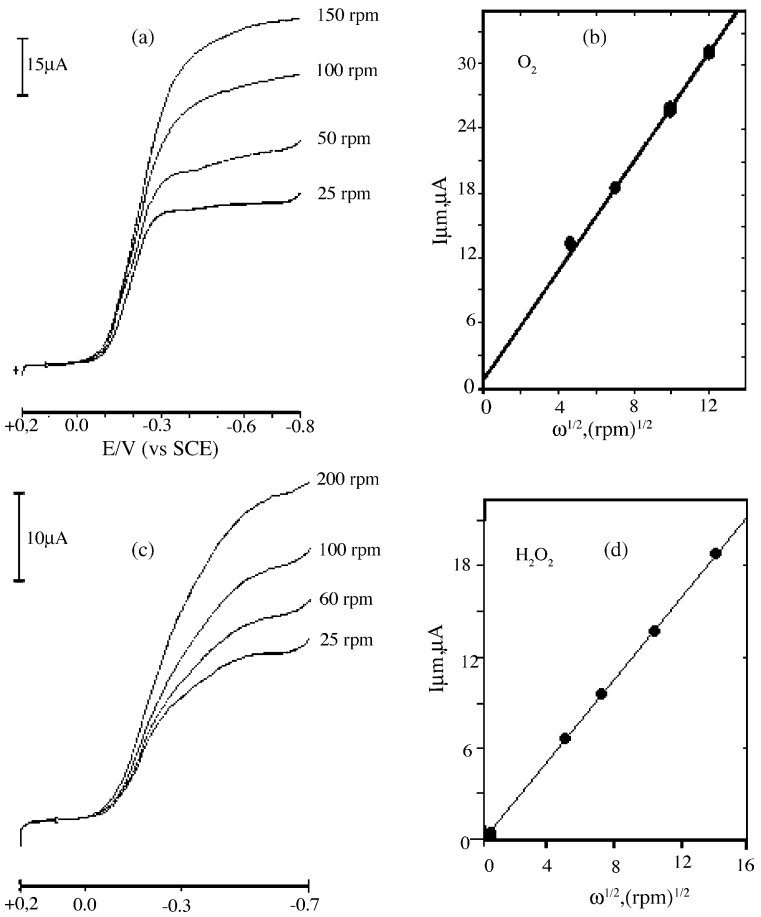

Fig. 7. Current–potential curves for O_2 (a) and H_2O_2 (c) reductions electrocatalyzed by a Cu(II)–TPT complex adsorbed on the graphite electrode, recorded at various electrode rotating rates as marked beside each curve. Koutecky–Levich plots for O_2 (b) and H_2O_2 (d) reductions, the data from (a) and (c), respectively. Other experimental conditions are as in Fig. 6.

order of 1. The pH dependences of I_k were also obtained as shown in Fig. 8 for O_2 (b) and H_2O_2 (d), respectively. It can be seen that I_k for O_2 and H_2O_2 reduction were independent of the solution pH, from which the zero reaction order of proton can be concluded. From the data shown in Fig. 8, the rate constants of O_2 and H_2O_2 reductions were estimated. They are listed in Table 1 (O_2) and Table 2 (H_2O_2).

Tables 1 and 2 show that the rate constant for the reduction of O_2 to water is almost five times faster that the reduction of H_2O_2 to water. Similar observations have also been reported for the reduction of H_2O_2 and O_2 catalyzed by a Cu(II) complex of 4,7-diphenyl-1,10-phenanthrolinedisulfonate adsorbed on a graphite surface [5,7].

Table 2
Rate constants for H_2O_2 reduction catalyzed by Cu(II)–TPT/electrode at 25 °C and 1.0 atm

$C(H_2O_2)$ ($\times 10^4$ mol dm^{-3})	I_k (μA)	$k(H_2O_2)$ ($\times 10^{-5}$ mol^{-1} dm^{-3} s^{-1})
2.2	2.0	1.9
2.6	3.0	2.4
4.3	4.6	2.2
6.5	7.6	2.4

The Cu(II)–TPT surface concentration is 7.5×10^{-10} mol cm^{-2}.

3.4. Proposed mechanism for the electrocatalyzed reductions of O_2 and H_2O_2

The pH dependencies of the potentials where the catalyzed reductions of O_2 and H_2O_2 proceed are shown in Fig. 9. The values plotted are the half-wave potentials of the reduction waves obtained at a rotating disk electrode. Compared with the pH dependency of the formal potential of waves III/III′ in Fig. 4(c), it can be seen that the half-wave potentials for the reduction of O_2 and H_2O_2 were more negative than those where the adsorbed Cu(II)–TPP complex was reduced to Cu(I)–TPT. The pH dependent pattern shown in Fig. 4(c) and Fig. 9 provides an insight into the mechanism of the electrocatalytic process. A deep analysis of the process has been reported in the literature [7]. The Cu(I)–TPT surface complex formed by the reduction of adsorbed Cu(II)–TPT on the electrode surface is believed to be the active catalyst which undergoes the inner-sphere mechanism for O_2 or H_2O_2 reduction. In this inner-sphere mechanism, the first step is the formation of an O_2 or H_2O_2 adduct:

$$[\mathrm{Cu(I)TPT(H2O)}]^+ + \mathrm{O_2} \rightarrow [\mathrm{Cu(I)TPT(O_2)}]^+ + \mathrm{H_2O} \quad (\text{for } \mathrm{O_2} \text{ reduction}) \qquad (6)$$

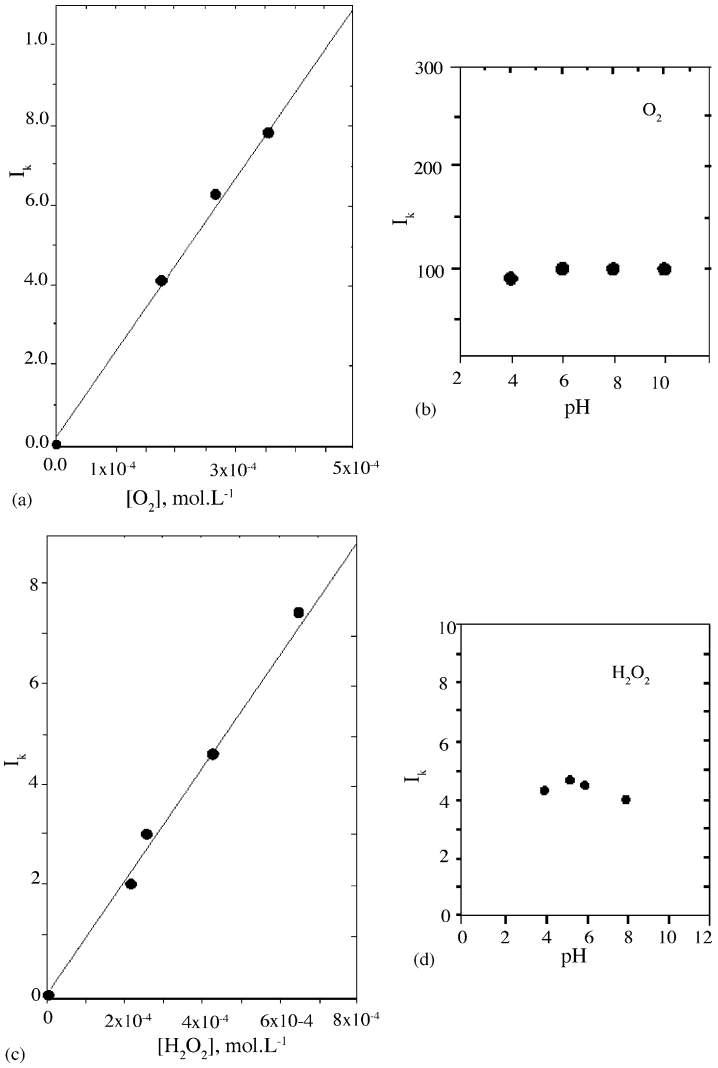

Fig. 8. O_2 (a and b) and H_2O_2 (c and d) concentration and pH dependencies of the kinetic current. The experimental conditions are as in Fig. 7.

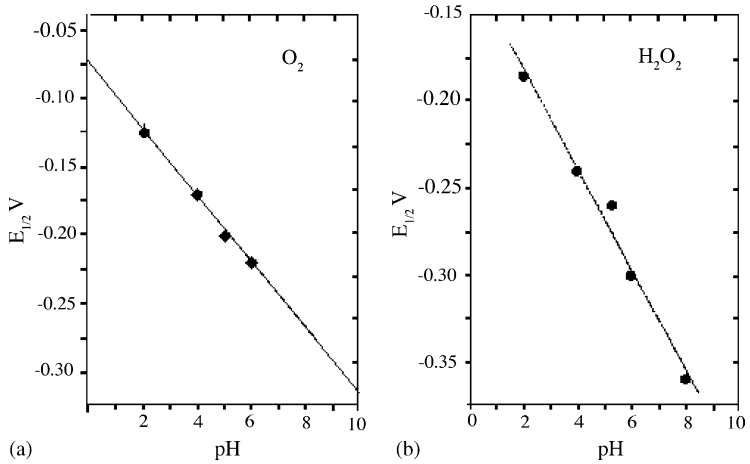

Fig. 9. pH dependencies of the half-wave potential for O_2 (a) and H_2O_2 (b) reductions catalyzed by adsorbed Cu(II)–TPT on the graphite electrode. Electrode rotating rate is 50 rpm, potential scan rate is 20 mV cm^{-1}. Other experimental conditions are as in Fig. 2.

or

$$[Cu(I)TPT(H_2O)]^+ + H_2O_2 \rightarrow [Cu(I)TPT(H_2O_2)]^+ + H_2O \quad (\text{for } H_2O_2 \text{ reduction}) \tag{7}$$

followed by electron transfer from bound O_2 to the electrode through the catalyst to form the final product H_2O under reductive polarization by the electrode:

$$[Cu(I)TPT(O_2)]^+ + 4H^+ + 4e^- \rightarrow [Cu(I)TPT(H_2O)]^+ + H_2O \quad (\text{for } O_2 \text{ reduction}) \tag{8}$$

or

$$[Cu(I)TPT(H_2O_2)]^+ + 2H^+ + 2e^- \rightarrow [Cu(I)TPT(H_2O)]^+ + H_2O \quad (\text{for } H_2O_2 \text{ reduction}) \tag{9}$$

The regenerated $[Cu(I)TPT(H_2O)]^+$ will participate in another cycle of the catalytic process. More experimental data are necessary for a detailed assessment of the proposed mechanism.

4. Conclusion

O_2 and H_2O_2 reductions electrocatalyzed by a copper–TPT complex adsorbed on the graphite electrode were investigated by cyclic voltammetry and a rotating disk electrode. The corresponding kinetic constants were obtained. The inner-sphere mechanism was employed to propose the reduction mechanism. In this inner-sphere mechanism, the adduct formation between the reactant (O_2 or H_2O_2) and surface Cu(I) center is believed to be the first step, which is followed by a four-electron transfer from bound O_2 to the electrode through the catalyst to form water (or by a two-electron process from H_2O_2 to water).

The surface coordination between adsorbed TPT and Cu(II) or Cu(I) was also investigated and evidenced by the solution UV–vis spectroscopic measurement for the Cu(II)–TPT complex. The coordination structures of Cu(II)–TPT and Cu(I)–TPT complexes were also proposed based on the experimental data.

The adsorbed TPT ligand displayed two successive reduction waves. The first wave (wave I) was identified as a two-electron and two-proton process, and the second wave (wave II) as a four-electron and four-proton process. The whole six-electron/six-proton process reduced the central conjugated triazine ring to a saturated C–N six-member ring.

Acknowledgements

Thanks to the CTPETRO (Edital CNPq/FINEP 03/2001), UFMA (Universidade Federal do Maranhão, Brazil) and FAPEMA for the scholarship grant. J. Zhang acknowledges the National Research Council Canada (NRC).

References

[1] J. Labuda, Anal. Chim. Acta 45 (4) (1990) 629.
[2] C. Shi, F.C. Anson, Inorg. Chem. 29 (1990) 4298.
[3] J.J. Zhang, F.C. Anson, J. Electroanal. Chem. 331 (1992) 945.
[4] A.L.B. Marques, J.J. Zhang, A.B.P. Lever, J. Pietro, J. Electroanal. Chem. 392 (1995) 43.
[5] J.J. Zhang, F.C. Anson, J. Electroanal. Chem. 341 (1992) 323.
[6] J.J. Zhang, F.C. Anson, Inorg. Chem. 33 (1994) 1392.
[7] J.J. Zhang, F.C. Anson, J. Electroanal. Chem. 348 (1993) 81.
[8] J.J. Zhang, F.C. Anson, J. Electroanal. Chem. 38 (1993) 2423.
[9] A.G. Fogg, R. Ismail, A. Rahim, H. Yusoff, R. Ahmad, F.G. Banica, Talanta 44 (03) (1997) 497.
[10] J. Barek, A.G. Fogg, J.C. Moreira, V.B. Zanini, J. Zima, Anal. Chim. Acta 320 (1) (1996) 31.
[11] J. Skopalova, M. Koutoucek, Fresenius J. Anal. Chem. 351 (7) (1995) 650.
[12] S.J. Liu, C.H. Huang, C.C. Chang, Mater. Chem. Phys. 82 (2003) 551.
[13] E.P. Marques, J.J. Zhang, Y.H. Tse, R.A. Metcalfe, W.J. Pietro, A.B.P. Lever, J. Electroanal. Chem. 395 (1995) 133.
[14] M.M. Kamal, A.Z. Zuhri, A.A.O. Nasser, Fresenius J. Anal. Chem. 356 (1996) 500.